ELSEVIER

PII: S0032-3861(96)01077-4

Polymer Vol. 38 No. 18, pp. 4571–4575, 1997

0032-3861/97/$17.00+0.00

polymer papers

SAXS measurements of the interface in polyacrylate and epoxy interpenetrating networks with fractal geometry

Susheng Tan*, Donghua Zhang and Enle Zhou
Polymer Physics Laboratory, Changchun Institute of Applied Chemistry, Chinese Academy of Sciences, Changchun 130022, P.R. China
(Received 28 August 1996; revised 8 November 1996)

The interface thickness in two-component interpenetrating polymer networks (IPN) system based on polyacrylate and epoxy were determined using small-angle X-ray scattering (SAXS) in terms of the theory proposed by Ruland. The thickness was found to be nonexistent for the samples at various compositions and synthesized at variable conditions—temperature and initiator concentration. By viewing the system as a two-phase system with a sharp boundary, the roughness of the interface was described by fractal dimension, D, which slightly varies with composition and synthesis condition. Length scales in which surface fractals are proved to be correct exist for each sample and range from 0.02 to 0.4 $Å^{-1}$. The interface in the present IPN system was treated as fractal, which reasonably explained the differences between Porod's law and experimental data, and gained an insight into the interaction between different segments on the interface.

(Keywords: SAXS; IPN; interphase)

INTRODUCTION

Recently, more and more attention was paid to fractals of objects in different fields[1]. A fractal object is defined as one which shows self-similarity over a range of length scales and a very simple power-law relation between the magnitude of a measureable property and the size of yardstick used to measure the property exists. The main research dealt with the theoretical properties of fractal objects and finding real physical systems with fractal behaviour. Many methods based on fractal concepts were used in experiments[2]. Scattering techniques, such as small-angle X-ray scattering (SAXS), small-angle neutron scattering (SANS) and Raman scattering, has been employed in several investigations of porous materials, silicas, coals, and aerogels, etc., including the determination of particle and pore size distribution and giving information about the fractal structure in these materials. A fractal interpretation was given by Spence and Elliot[3] after analysing small-angle X-ray-scattering data from obliquely evaporated amorphous chalcogenide films. In this work, SAXS was used to obtain the interphase information in interpenetrating polymer networks.

Interpenetrating polymer networks (IPNs) have created more and more interest due to their excellent properties; the relationship of the properties to the multiphase morphology has been investigated for many years. Because of thermodynamic immiscibility, IPNs usually exhibit a multiphase structure at room temperature. This has been determined by a number of researchers from TEM photographs. A three-phase system is often observed due to the interpenetration between the two or more polymer networks in IPNs. The third phase is the interphase which consists of both components. The interphase is very sensitive to interpenetration. Usually, the more the interpenetration, the thicker the interphase[4].

SAXS is a useful experiment method in the determination of morphology of multiphase polymer materials such as semi-crystalline polymer, polymer blends, etc. Especially, SAXS has been used to obtain information about the interphase and define its thickness in IPNs[5]. We have used it to study the multiphase morphology of PEGDA/DGEBA IPNs and obtained a satisfactory result which is in agreement with the results obtained by TEM, d.m.a., etc.[6]. When the SAXS data of IPNs were analysed, the interphase between the two phases was usually viewed as a smooth surface with thickness E. In contrast, in this paper we have detected the interface irregularity in IPNs by contemplating the interface as a fractal one.

EXPERIMENTAL

Preparation of the IPN's sample

The IPNs of polyacrylate [poly(polyethylene glycol diacrylate), PEGDA] and epoxy (diglycidyl ether of bisphenol A, DGEBA) were prepared simultaneously with 2,2′-azobisisobutyronitrile (AIBN) as the initiator of PEGDA and xylydene amine (XLA) as the solidifying catalyst of DGEBA. The synthesis parameters are listed in *Table 1*. The detailed procedures of the synthesis of PEGDA and IPNs were described previously[7,8].

* To whom correspondence should be addressed

Table 1 Synthesis parameters, fractal dimension D and length scales for PEGDA/DGEBA IPNs[a]

Sample No.	PEGDA/ DGEBA	% AIBN	T(K)	D^b	D^c	q_{min}(Å^{-1})	q_{max}(Å^{-1})
1	75/25	0.40	333	2.52	2.51	0.032	0.254
2	50/50	0.40	333	2.53	2.52	0.039	0.252
3	25/75	0.40	333	2.48	2.47	0.030	0.250
4	50/50	0.20	333	2.94	2.93	0.024	0.240
5	50/50	0.60	333	2.70	2.69	0.029	0.323
6	50/50	0.40	348	2.65	2.64	0.038	0.285
7	50/50	0.40	363	2.78	2.77	0.032	0.340

[a] The number of the SAXS curves of all samples are 3, and the D value error is from 0.08 to 0.15
[b] Determined according to equation (11)
[c] According to equation (10)

SAXS experiments

The SAXS intensity of the samples were registered with a Kratky compact camera, the front of which was directly mounted on the top of the cube shield of a stabilized Philips PW1170 X-ray generator. The Kratky X-ray tube was operated at a power of 1.5 kW. Cu $K\alpha$ radiation was used; the monochromatization was performed by an Ni filter in conjunction with a pulse-height discriminator. Measurements were made by a step-scanning procedure and in the fixed time mode, with a sampling time of 200 s for each step. The number of steps was generally of the order of 250 for each sample. The entrance and detector slits were adjusted respectively to 80 and 200 μm. However, to approach the origin of the angles as closely as possible, the beginning of the curve was also registered with the entrance and detector slits adjusted to 42.5 and 107.5 μm and then merged with the main part of the curve. The explored domain was thus 0.006 nm^{-1}, where $s = 2\sin\theta/\lambda$, 2θ is the scattering angle and λ is the X-ray wavelength (1.542 Å). Absorption, sample thickness, parasitic intensity and electronic noise were taken into account in the standard manner. The scattering geometry used was in the finite-slit-height mode where the width of the incident beam was comparable to the width of the receiving slit. Corrections were made for the slit-smearing effect with a method proposed by Strobl[9].

RESULTS AND DISCUSSION

At first sight, the experimental data are quite similar for those PEGDA/DGEBA IPNs synthesized at various conditions as was expected. They all show a regular decay followed by an important increase in the scattering at high angles which characterizes a background associated with density fluctuations within the phases or thermal density fluctuations. In the following description of the experimental data, the results of PEGDA/DGEBA IPNs with various compositions are described in detail, and the description of the other four IPNs prepared at variable conditions, which have similarity with the former, are not given. We only offer their ultimate results and conclusions, namely the fractal dimensions and the length scales.

Determination of the interphase thickness

According to Porod's law, the intensity in the tail of the SAXS curve of structures with sharp phase boundaries decreases in proportion to s^{-4} [10–12]. However, polymers often exhibit systematic deviation from Porod's law, that is, the product of $I_{(s)}s^4$ does not reach a constant value. This behaviour may be interpreted in terms of the detailed microstructure of the polymer. The presence of thermal density fluctuations or mixing within phases results in an enhancement of scattering at high angles causing a plot of $I_{(s)}s^4$ vs. s^2 to have a positive slope. Consequently, these effects are known as positive deviations from Porod's law. On the other hand, the existence of a diffuse phase boundary causes a depletion of high-angle scattering resulting in a negative slope for such a plot. Hence, these effects are referred to as negative deviations from Porod's law[13,14].

Thanks to the positive and negative deviations, the scattering intensity in the Porod's region is given by

$$I_{obs(s)} = I_{(s)}H^2_{(s)} + I_{B(s)} \quad (1)$$

The form of the smoothing function used is dependent on the geometrical model for the interphase gradient. In the present paper, the sigmoidal-gradient model is employed, thus the smoothing function is Gaussian and $H_{(s)}$ is given by[15,16]

$$H_{(s)} = \exp(-2\pi^2\sigma^2 s^2) \quad (2)$$

where σ is the standard deviation of the Gaussian smoothing function and is a measure of the transition-layer width.

There are several factors which give rise to a scattering background and lead to positive deviations from Porod's law. These deviations have been treated by Rathje and Ruland[17], Wiegand and Ruland[18], and Vonk *et al.*[19].

Ruland's method is based on the approximation of the background intensity as an exponential[14]

$$I_{B(s)} = Fl\exp(b_2 s^2) \quad (3)$$

where b_2 is a constant and Fl is the intensity value extrapolated to zero angle. In our present work, the wide-angle data were obtained, if the intensities are absolute, the value of Fl (corrected for slit-smearing) reflects the magnitude of the thermal density fluctuations. In *Figure 1*, the logarithm of the smeared intensity ($I_{(s)}$) obtained from PEGDA/DGEBA IPNs with various compositions is plotted against s^2, the linear relation exhibited by the larger angle data indicates the validity of equation (3). As described above, the other PEGDA/DGEBA IPNs synthesized at different conditions have the same results. Namely, the smeared intensity obtained from PEGDA/DGEBA IPNs synthesized at different

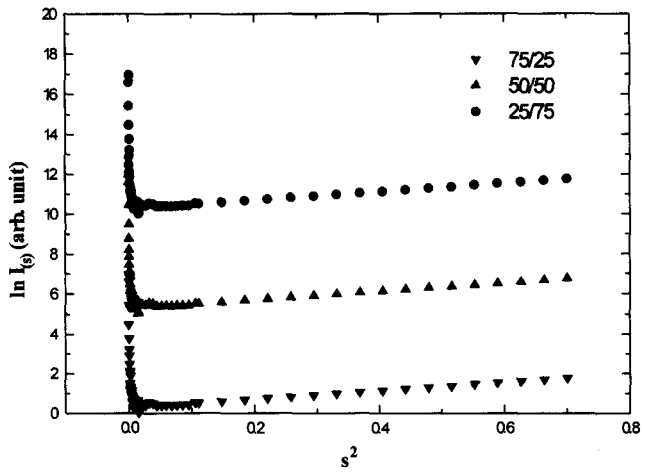

Figure 1 Slit-smeared intensities $I_{(s)}$ obtained with PEGDA/DGEBA IPNs plotted semilogarithmically against s^2 to illustrate that the tail of the scattering curves can be approximated well by $\exp(bs^2)$

temperatures and various initiator concentrations all shows a linear relation at the large angle by logarithm of $I_{(s)}$ against s^2.

The scattering intensity in the Porod region after removing contributions of backgrounds, that is the corresponding Porod-law relation, becomes

$$I_{\text{obs}(s)} = (K_p/s^4)\exp(-4\pi^2\sigma^2 s^2) \quad (4)$$

By expanding the exponential function the intensity may be approximated by

$$I_{\text{obs}(s)} = (K_p/s^4)(1 - 4\pi^2\sigma^2 s^2) \quad (5)$$

Practically, the smeared data can be used only if the effect of the oscillation of slit on scattering intensity, thus the smeared scattering intensity of the sigmoidal-type system adjusted by infinite-height slit, I_{smeared}, can be given by [20]

$$I_{\text{smeared}(s)} = (K_p/s^3)(1 - 4\pi^2\sigma^2 s^2) \quad (6)$$

Koberstein *et al.*[15] proposed a method which can be directly applied to smeared intensity and has a relatively large range of applicability. They find that the smeared intensity obtained with an infinite-slit geometry can be represented by an excellent approximation, up to a much larger value of s, by

$$I_{\text{smeared}(s)} = K' s^{-3}\exp[-38(\sigma s)^{1.81}] \quad (7)$$

where 38 and 1.81 are empirically determined constants. One may plot $\ln[I_{(s)}s^3]$ vs. $s^{1.81}$ to evaluate the interphase parameter, σ, as $[-(\text{slope})/38]^{1/1.81}$ or plot $s^{-1.81}\ln[I_{(s)}s^3]$ vs. $s^{-1.81}$ to evaluate σ as $[-(\text{intercept})/38]^{1/1.81}$.

In all scattered intensity data shown hereafter, the observed intensity has been corrected for the background for subtracting the contribution of the thermal density fluctuation as given by equation (3). Other methods to subtract the background proposed by Vonk *et al.* can be chosen. However, the manner of subtracting the background scattering did not much affect the final value of the interphase thickness according to Hashimoto *et al.*[21].

Plots of $s^{-1.81}\ln[I(s)s^3]$ vs. $s^{-1.81}$ are shown in *Figure 2*. According to equation (7), this plot should give a negative intercept for PEGDA/DGEBA IPNs with a diffuse domain boundary. However, positive intercepts are shown for all PEGDA/DGEBA IPNs. This implies that the domain boundaries are very sharp in this system studied here. Several measurements at the same condition have failed to obtain interphase thickness in these IPNs. Careful examination shows that estimates of the background contribution are proper. Linear regresses of $\ln[I_{(s)}]$ vs. s^2 in the large s region are of correlation coefficients over 0.98, as shown in *Figure 1*. Therefore, the positive intercepts shown in *Figure 2* do not result from the lower estimate of the background contribution.

Plots of $\ln[I_s s^4]$ vs. s^2 for desmeared scattering data are shown in *Figure 3*. According to equation (4), such plots will give negative slopes for IPNs with diffuse domain boundaries, and the interphase thickness can be estimated from $[-(\text{slope})/4\pi^2]^{1/2}$. However, the plots result in positive slopes, implying sharp interphase in the system.

Summarizing the results obtained by the two different methods of evaluating the interphase thickness parameter, σ, in PEGDA/DGEBA IPNs, we can say that the samples studied here are of sharp domain boundaries. σ obtained from *Figure 2* is negative, and does not have

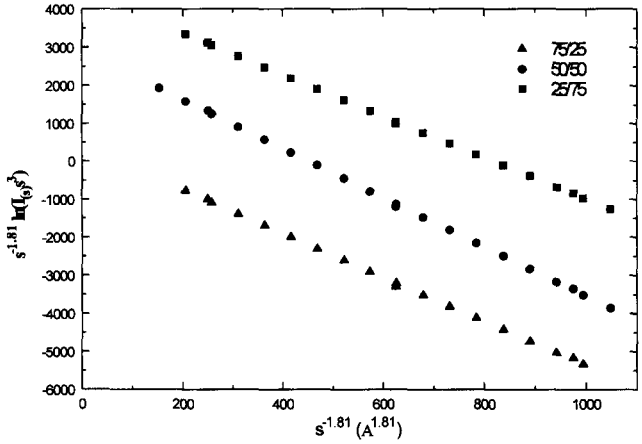

Figure 2 Plot to evaluate the interfacial thickness parameter σ according to equation (7). $s^{-1.81}\ln(s^3 I)$ (with I from which the background, I_b, has been subtracted) is plotted against $s^{-1.81}$. σ is evaluated as $[-(\text{intercept})/38]^{1/1.81}$. For the sake of clarity, the data point for 50/50 and 25/75 PEGDA/DGEBA IPNs are displaced upward respectively

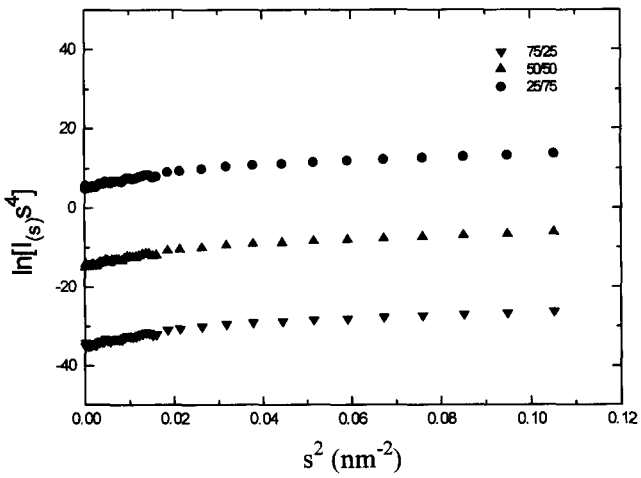

Figure 3 Plot to evaluate the interfacial thickness parameter, σ according to equation (5). $\ln(s^4 I)$ (with I from which the background, I_b, has been subtracted) is plotted against s^2. For the sake of clarity, the data point for 50/50 and 25/75 PEGDA/DGEBA IPNs are displaced upward respectively

physical meaning. Thus, if the interphase in these IPNs exists, the thickness should be zero. It seems that the theory proposed by Ruland *et al.* cannot be applied to this IPN system. In the next section, a fractal description of the interface is proposed and found to be of definite physical meaning.

Fractal behaviour of the interphase

Deviations from Porod's law have also been found in PEGDA/DGEBA IPNs, which have been discussed fully above. Until recently, Bale and Schmidt[22] outlined some equations for analysis of X-ray scattering data in the large-q region by considering the coal pore surfaces to be fractal. They showed that fractal surfaces with dimension $D > 2$ had a correlation function of the form:

$$g(r) = 1 - cr^{3-D} \tag{8}$$

where $c = (N_0/4)[I/v\phi(1-\phi)]$, v is the sample volume. ϕ is the porosity (volume fraction of the pores), N_0 is a constant which depends on the fractal geometry, and D is the fractal dimension. Substituting $g(r)$ into the general form of the SAXS intensity equation, we can get

$$I(q) = 4\pi I_e \delta^2 v\phi(1-\phi)\int_0^\infty r^2 g(r)\sin(qr)/(qr)\,dr \tag{9}$$

where δ is the uniform electron density of the porous solid, and q is another form of the scattering vector, which is equal to $4\pi\sin\theta/\lambda$. In the large q region, it gives

$$I(q) \propto q^{D-6} \qquad (D < 6) \tag{10}$$

According to this approximation, when the surface is smooth ($D = 2$), $I(q)$ is proportional to q^{-4}, which is exactly the Porod situation.

Equation (10) can only be applied to the desmeared scattering intensity. The desmearing introduces inaccuracies involved with data extrapolation beyond measurable angles and serious amplification of statistical errors in photon counting. For these reasons, it is desirable to develop smeared relations which may be applied directly to smeared intensity data from fractal objects. After smearing the theoretical relations of equation (10), we can get

$$I_\infty(q) \propto q^{D-5} \tag{11}$$

where $I_\infty(q)$ is the smeared intensity measured by the infinite-length collimation system. For certain slit geometries, as in the Kratky camera, the infinite-length assumption may be employed[23]. However, the trapezoidal weighting function, which can be calculated from the experimental geometry, is often used to describe the Kratky camera. In this case, one expects

$$I_{tr}(q) = I_\infty(q)\{(2-\beta)\,\mathrm{tg}^{-1}[(2-\beta)/t] - \beta\,\mathrm{tg}^{-1}(\beta/t)\}/[(1-\beta)] \tag{12}$$

where $I_{tr}(q)$ is the intensity measured by the Kratky camera, $I_\infty(q)$ is the intensity measured with the infinite-length collimation system, and $t = 2h/(A+B)$, $\beta = 2A/(A+B)$, with h the angular distance from the primary beam, A and B are the parameters characterizing the shape of the primary intensity profile, which is equal to $0.052\,\text{Å}^{-1}$ and $0.1\,\text{Å}^{-1}$ in our present work, respectively[24]. Therefore, the measured intensity with the Kratky camera can be thus related to the $I_\infty(q)$ where equation (11) is applied. In this paper, all the scattering data measured by Kratky camera have been transferred into $I_\infty(q)$ by equation (12) in order to deduce results from equation (11).

When PEGDA/DGEBA IPN system is viewed as a two-phase system with sharp, rough boundaries, the power-law proposed by Porod is no longer suitable. For these composites, rough interface, a fractal description may be appropriate. Equations (10) and (11) can be adapted for analysis of SAXS data from PEGDA/DGEBA IPNs. In *Figure 4*, the plots of smeared intensity $\ln[I(q)]$ vs. $\ln q$ are represented. Straight lines are obtained for each specimen at every composition and at every variable synthesis condition over a relatively wide range of q. According to equation (11), the value of D, the fractal dimension of the interface, can be found from the line slope. These fractal dimensions (D) are listed in *Table 1*.

Plots of the desmeared intensity $\ln[I(q)]$ vs $\ln q$ are represented in *Figure 5*. Straight lines are obtained for the samples at every composition and at every various synthesis condition. The fractal dimension D obtained from fits of equation (10) to the desmeared scattering data is also listed in *Table 1*. Comparing the values of D obtained from different methods, we find that they are agreeable within the experimental errors.

Summarizing the results above, a fractal description of the interface in PEGDA/DGEBA IPNs used here do have definite physical meaning. The fractal dimension D and the length scales in which D exists describe the

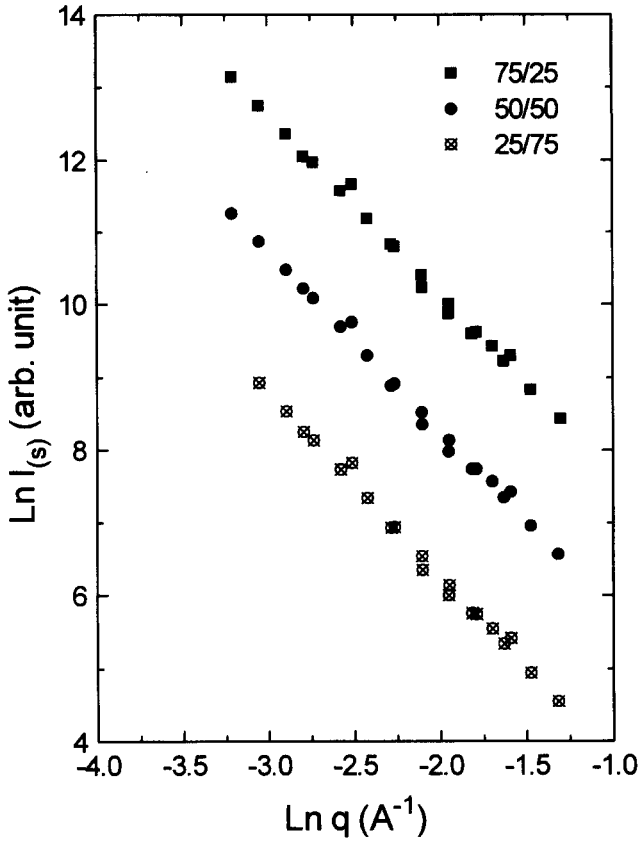

Figure 4 Ln–ln plot of slit-smeared intensities I from which the background, I_b, has been subtracted as q to show the linear relationship between ln I and ln q according to equation (11). For the sake of clarity, the data points for 50/50 and 25/75 PEGDA/DGEBA IPNs are displaced downward respectively

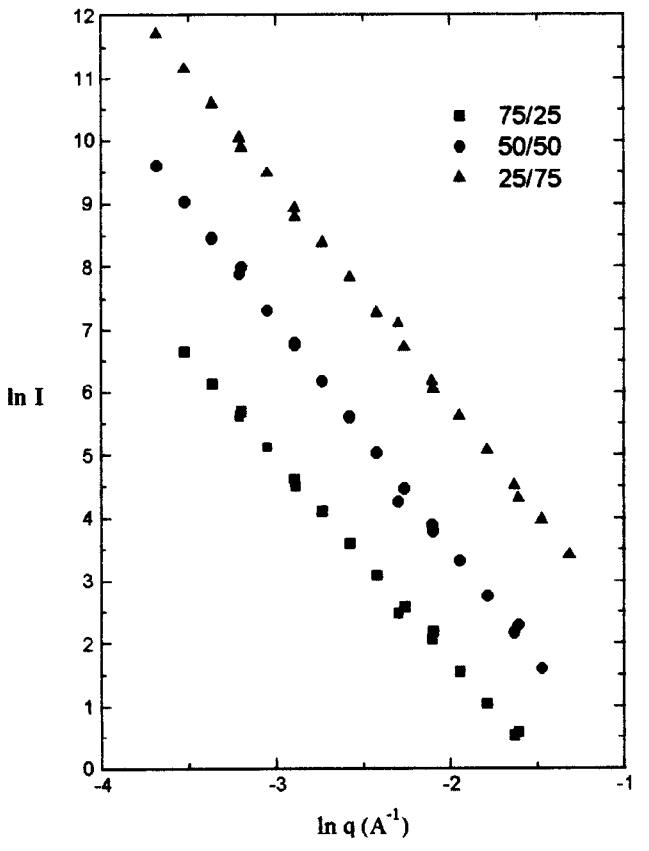

Figure 5 Ln–ln plot of desmeared intensities I against q to show the linear relationship between ln I and ln q according to equation (10). For the sake of clarity, the data points for 50/50 and 75/25 PEGDA/DGEBA IPNs are displaced downward respectively

interface sharpness, roughness, and the interaction between different segments. These results are consistent with the general model of IPN structures as revealed by other physical or chemical techniques.

Moreover, samples with various compositions show slight discrepancy in fractal dimension and length scales, which represent the similarity of their interphase in the fractal domain. The case of samples synthesized at variable AIBN concentrations is very interesting. Sample 2, which has the smallest fractal dimension value compared with samples 4 and 5, is the one which repre-sents the least rough fractal interphase. While, in the case of samples synthesized at different temperatures, sample 7 has the highest value compared with samples 2 and 6 in fractal dimension which give rise to the roughest interphase between the two component domains.

CONCLUSIONS

Ruland's theory was applied to analyse the SAXS data for PEGDA/DEGBA IPN system. The interphase thickness was probed. It was found that the interphase thickness did not exist in this system. The results imply that the interface is very sharp. Because of this, a fractal concept was introduced to study the scattering behaviour of a rough interface with sharp boundaries. Results show that there are length scales where the scattering data follow surface fractal power laws other than Porod's law. The interface in this PEGDA/DGEBA IPN system was found with fractal properties. The fractal dimension changes from sample to sample and varies with compositions and synthesis conditions.

ACKNOWLEDGEMENT

The financial support of the National Natural Science Foundation of China is gratefully acknowledged.

REFERENCES

1. Mandelbrot, B. B., *The Fractal Geometry of Nature*. Freeman, San Francisco, 1983.
2. Fairin, D., Peleg, S., Yavin, D. and Avnir, D., *Langmuir*, 1985, **1,** 399.
3. Spence, G. A. and Elliot, S. R., *Solid State Commun.*, 1989, **79,** 1035.
4. Sperling, L. H., *Interpenetrating Polymer Networks and Related Materials*. Plenum Press, New York, 1981.
5. Lipatov, Y. S., Shilov, V. V. and Bogdanovich, V. A. *et al.*, *J. Polym. Sci. Polym. Phys. Ed.*, 1987, **25,** 1903.
6. Tan, S., Zhang, D. and Zhou, E., *Polym. Int.*, 1997 (in press).
7. Tan, S., Zhang, D. and Zhou, E., *Polym. Networks Blends*, 1996, **6,** 91.
8. Tan, S. and Zhang, D., *Acta Polymerica*, 1996, **47,** 219.
9. Strobl, G. R., *Acta Crystallogr.*, 1970, **A26,** 367.
10. Kratky, O., *Pure Appl. Chem.*, 1966, **12,** 483.
11. Vonk, C. G., *J. Appl. Cryst.*, 1971, **4,** 340.
12. Porod, G., *Kolloid Z.*, 1952, **125,** 51.
13. Porod, G., *Kolloid Z.*, 1952, **125,** 108.
14. Ciccariello, S. *et al.*, *J. Appl. Cryst.*, 1988, **21,** 117.
15. Koberstein, J. T., Morra, B. and Stein, R. S., *J. Appl. Cryst.*, 1980, **13,** 34.
16. Ruland, W., *J. Appl. Cryst.*, 1971, **4,** 70.
17. Bonart, R. and Muller, E. H., *J. Macromol. Sci. Phys.*, 1974, **B10,** 177.
18. Rathje, J. and Ruland, W., *Colloid Polym. Sci.*, 1976, **254,** 358.
19. Wiegand, W. and Ruland, W., *Prog. Colloid Polym. Sci.*, 1979, **66,** 355.
20. Kawaguchi, T. and Hamenda, T., *J. Appl. Cryst.*, 1992, **25,** 778.
21. Hashimoto, T., Todo, A., Itoi, H. and Kawai, H., *Macromolecules*, 1977, **10,** 377.
22. Bale, D. and Schmidt, P. W., *Phys. Rev. Lett.*, 1984, **53,** 596.
23. Ruland, W., *J. Appl. Crystallogr.*, 1974, **7,** 383.
24. Xie, R., Yang, B. and Jiang, B., *Phys. Rev. B*, 1994, **50,** 3636.